Exact Minkowski Products of N Complex Disks

RIDA T. FAROUKI
Department of Mechanical and Aeronautical Engineering, University of California, Davis, CA 95616, USA, e-mail: farouki@ucdavis.edu

and

HELMUT POTTMANN
Institut für Geometrie, Technische Universität Wien, Wiedner Hauptstrasse 8–10, A–1040 Wien, Austria, e-mail: pottmann@geometrie.tuwien.ac.at

Abstract. An exact parameterization for the boundary of the Minkowski product of N circular disks in the complex plane is derived. When $N > 2$, this boundary curve may be regarded as a generalization of the Cartesian oval that bounds the Minkowski product of two disks. The derivation is based on choosing a system of coordinated polar representations for the N operands, identifying sets of corresponding points with matched logarithmic Gauss map that may contribute to the Minkowski product boundary. By means of inversion in the operand circles, a geometrical characterization for their corresponding points is derived, in terms of intersections with the circles of a special coaxal system. The resulting parameterization is expressed as a product of N terms, each involving the radius of one disk, a single square root, and the sine and cosine of a common angular variable φ over a prescribed domain. As a special case, the N-th Minkowski power of a single disk is bounded by a higher trochoid. In certain applications, the availability of exact Minkowski products is a useful alternative to the naive bounding approximations that are customarily employed in "complex circular arithmetic."

1. Preamble

Minkowski geometric algebra [11], [12] is concerned with the complex sets[*]

$$\mathcal{A} \oplus \mathcal{B} = \{\mathbf{a} + \mathbf{b} \mid \mathbf{a} \in \mathcal{A} \text{ and } \mathbf{b} \in \mathcal{B}\},$$
$$\mathcal{A} \otimes \mathcal{B} = \{\mathbf{a} \times \mathbf{b} \mid \mathbf{a} \in \mathcal{A} \text{ and } \mathbf{b} \in \mathcal{B}\}, \tag{1.1}$$

populated by sums or products of pairs of complex numbers $\mathbf{a}$ and $\mathbf{b}$, chosen independently from given complex-set operands $\mathcal{A}$ and $\mathcal{B}$. The scope of this algebra may be profitably extended to encompass Minkowski powers, roots, sets defined by bivariate functions $\mathbf{f}(\mathbf{a}, \mathbf{b})$ beyond $\mathbf{a} + \mathbf{b}$ and $\mathbf{a} \times \mathbf{b}$, and other operations: see [9], [11], [12] for further details, and a discussion of the diverse applications and interpretations of Minkowski geometric algebra.

---

[*] Following [11], [12] we shall denote real numbers by italic characters, complex numbers by bold characters, and sets of complex numbers by upper-case calligraphic characters.

Conceptually, Minkowski geometric algebra is the natural generalization of real *interval arithmetic* [22], [23] to complex-number sets. In the transition from real to complex, however, the trivial geometry of real intervals (and their consequent closure under addition and multiplication) must be relinquished. Even "simple" sets, such as rectangles or circular disks in the complex plane, do not exhibit closure under the Minkowski product operation.

Motivated by the study of polynomial root-finding algorithms, Gargantini and Henrici [13] introduced *circular complex arithmetic* as a practical means to cope with the increasing algebraic and geometrical complexity of successive complex-set operations. Each element of this system is a circular disk in the complex plane, specified by a center $\mathbf{c}$ and radius R. The Minkowski sum of two disks $(\mathbf{c}_1, R_1)$ and $(\mathbf{c}_2, R_2)$ is exactly $(\mathbf{c}_1 + \mathbf{c}_2, R_1 + R_2)$. However, instead of the exact Minkowski product (which is not a circular disk), this approach employs the *bounding disk* with center and radius

$$\mathbf{c} = \mathbf{c}_1 \mathbf{c}_2, \qquad R = |\mathbf{c}_1| R_2 + |\mathbf{c}_2| R_1 + R_1 R_2. \tag{1.2}$$

Although this is not the *smallest* disk that contains the Minkowski product, it has the virtue of being centered on the product $\mathbf{c}_1 \mathbf{c}_2$ of the operand centers. Hauenschild [16], [17] describes "optimal" circular arithmetic, based on the use of *minimal* bounding disks (which entail solving a cubic equation). Further details on complex circular arithmetic may be found in [1], [18], [26], [29].

Besides root-finding algorithms, the arithmetic of complex disks arises in the investigation of robust stability of dynamic systems, whose characteristic polynomials have uncertain coefficients given by disks in the complex plane [5], [27]. Another application is in the generalization of Bernstein–Bézier curve representations to "uncertainty disks" as control points [20].

In the "standard" case $\mathbf{c}_1 = \mathbf{c}_2 = 1$, expressions (1.2) clearly give $\mathbf{c} = 1$ and $R = R_1 + R_2 + R_1 R_2$. This result can be extended to more than two disks: for example, the product of three disks with center 1 and radii R_1, R_2, R_3 has center 1 and bounding radius

$$R = R_1 + R_2 + R_3 + R_1 R_2 + R_2 R_3 + R_3 R_1 + R_1 R_2 R_3. \tag{1.3}$$

As seen in Figure 1, the bounding disks defined by this "circular arithmetic" are sharp only for the maximum modulus of complex values belonging to the exact Minkowski products. In some applications, replacing exact Minkowski products by simpler bounding sets may be unsatisfactory (especially if these supersets become increasingly loose as successive operands are introduced).

Consider, for example, the following simple problem. We are interested in whether the polynomial $f(\mathbf{z}) = \mathbf{z}^2$ can assume the value 0 when the argument is selected from the complex disk $\mathcal{C}$ defined by $|\mathbf{z} - 1| \leq 3/4$. Circular complex arithmetic (based on bounding disks) indicates that this may be a possibility, but the exact Minkowski product $\mathcal{C} \otimes \mathcal{C}$ shows that it is impossible.
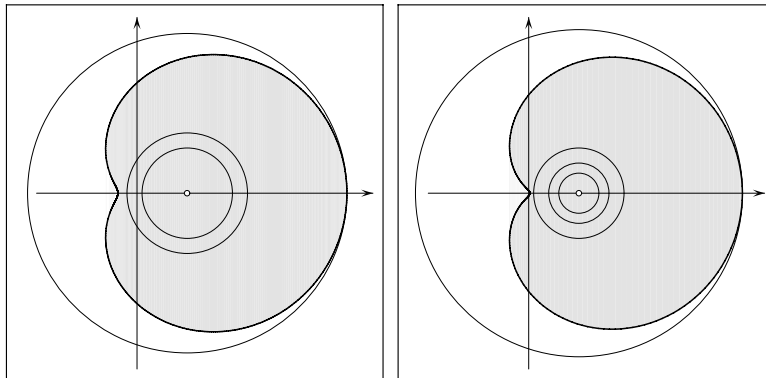
Figure 1. The Minkowski products (shaded areas) of two disks with $R_1 = 0.9$, $R_2 = 1.2$ (left), and of three disks with $R_1 = 0.4$, $R_2 = 0.6$, $R_3 = 0.9$ (right); also shown are circumferences of the bounding disks defined by (1.2) and (1.3).

The goal of this paper is to show that the Minkowski product of *N* disks admits an exact and relatively simple boundary description. Specifically, we shall derive a closed-form parameterization for the boundary involving only arithmetic operations, trigonometric functions in a single angular variable φ (restricted to an appropriate domain), and *N* square roots.

Our plan for the paper is as follows. In Section 2 we summarize some geometrical properties of Cartesian ovals, the curves that bound the Minkowski products of two complex disks. A coordinated parameterization for two circles is then derived in Section 3, based on matching their logarithmic Gauss maps, that induces a closed-form parameterization of their Minkowski-product boundary. In Section 4 we show that this approach admits a natural generalization (subject to some technical qualifications) to the Minkowski products of *N* disks. The special case of the *N*-th Minkowski power of a single disk is discussed in Section 5. Finally, in Section 6 we make some concluding remarks concerning the practical significance of these results, and identify some open theoretical problems.

2. Geometry of Cartesian ovals

Given complex domains $\mathcal{A}$ and $\mathcal{B}$ with regular boundary curves $\partial\mathcal{A}$ and $\partial\mathcal{B}$, the boundary of their Minkowski product $\mathcal{A} \otimes \mathcal{B}$ satisfies

$$\partial(\mathcal{A} \otimes \mathcal{B}) \subseteq (\partial\mathcal{A}) \otimes (\partial\mathcal{B}).$$

Thus, if $\mathcal{A}$ and $\mathcal{B}$ are circular disks, we are mainly concerned with Minkowski products of *circles*. We also recall [12] that, for non-zero complex numbers **p** and **q**, the Minkowski product satisfies

$$\mathcal{A} \otimes \mathcal{B} = \{\mathbf{pq}\} \otimes (\{\mathbf{p}^{-1}\} \otimes \mathcal{A}) \otimes (\{\mathbf{q}^{-1}\} \otimes \mathcal{B}).$$

Hence, for circular disks $\mathcal{A}$ and $\mathcal{B}$ with centers* $\mathbf{p} \neq 0$ and $\mathbf{q} \neq 0$, we may always consider the simpler equivalent problem of disks centered at the point 1 on the real axis, and radii scaled by the factors $|\mathbf{p}|^{-1}$ and $|\mathbf{q}|^{-1}$.

We have shown [12] that the Minkowski product of two circles $\mathcal{C}_1$, $\mathcal{C}_2$ with center 1 and radii R_1, R_2 is the region between the two loops of a *Cartesian oval*, an irreducible quartic curve [19], [21]. Moreover, as previously noted in [27], the Minkowski product of the circular disks $\mathcal{D}_1$, $\mathcal{D}_2$ bounded by $\mathcal{C}_1$, $\mathcal{C}_2$ is the region contained within the *outer* loop of the Cartesian oval.

Despite its key role in the Minkowski geometric algebra of complex sets, and in other areas such as geometrical optics [7], [8], the Cartesian oval remains a relatively obscure curve. Perhaps the most thorough description is given by Gomes Teixeira [14]. Since a complete understanding of its subtle geometry is essential to generalizing the Minkowski product of two circular disks to the case of N disks, we shall devote the remainder of this section to an elucidation of some key geometrical properties of the Cartesian oval.

2.1. BIPOLAR REPRESENTATION

The simplest characterization of Cartesian ovals employs bipolar coordinates. We may take the origin as one pole, and either of the points $a_1 = 1 - R_1^2$ and $a_2 = 1 - R_2^2$ on the real axis as the other. Then, writing

$$\rho_0 = \sqrt{x^2 + y^2}, \qquad \rho_1 = \sqrt{(x - a_1)^2 + y^2}, \qquad \rho_2 = \sqrt{(x - a_2)^2 + y^2}$$

for the distance of $\mathbf{z} = x + \mathrm{i}y$ from these poles, either of the bipolar equations

$$R_1\rho_0 \pm \rho_1 = \pm a_1 R_2 \qquad \text{or} \qquad R_2\rho_0 \pm \rho_2 = \pm a_2 R_1 \tag{2.1}$$

describes the Cartesian oval that bounds $\mathcal{C}_1 \otimes \mathcal{C}_2$. A third bipolar description may be given by choosing a_1 and a_2 as poles—the equation is then

$$R_2\rho_1 \pm R_1\rho_2 = \pm(a_1 - a_2). \tag{2.2}$$

By squaring to eliminate radicals, one can verify that the Cartesian oval described by each of the above bipolar equations is the quartic curve

$$(x^2 + y^2 - 2x + a_1 a_2)^2 - 4R_1^2 R_2^2 (x^2 + y^2) = 0. \tag{2.3}$$

This curve has double points at each of the circular points at infinity, and is therefore (in general) of genus 1. Degenerate instances of the Cartesian oval are as follows: (i) if $R_1 = 1 \neq R_2$, $R_1 \neq 1 = R_2$, or $R_1 = R_2 \neq 1$, we have a rational curve, the *limaçon of Pascal*, the two coincident poles corresponding to a node on the curve; and (ii) if $R_1 = R_2 = 1$, all three poles coincide and the node becomes a cusp, yielding a *cardioid* (see Figure 2).

---

* If (say) $\mathbf{p} = 0$, the Minkowski product $\mathcal{A} \otimes \mathcal{B}$ is trivial—it is simply the disk centered at the origin with radius $a(|\mathbf{q}| + b)$, where a and b are the radii of $\mathcal{A}$ and $\mathcal{B}$.
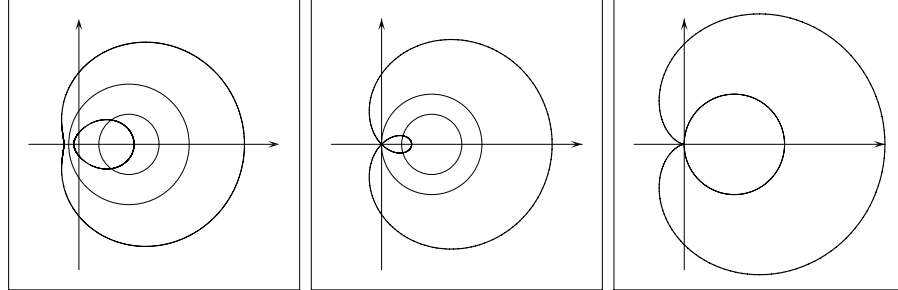
Figure 2. A Cartesian oval (left, with $R_1 = 0.5$, $R_2 = 1.2$), limaçon of Pascal (center, with $R_1 = 0.7$, $R_2 = 1$), and the cardioid (right, with $R_1 = R_2 = 1$).
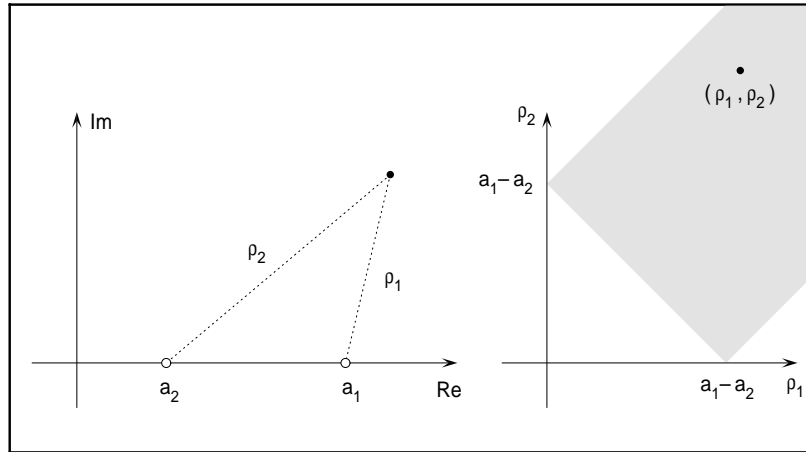
Figure 3. Bipolar coordinates (ρ_1, ρ_2) with respect to poles $\mathbf{p}_1 = (a_1, 0)$ and $\mathbf{p}_2 = (a_2, 0)$—the region of valid ρ_1, ρ_2 values is shown shaded on the right.

Now although equations (2.1) and (2.2) admit four sign combinations, only two of them define real loci—the inner and outer loops of a Cartesian oval. To illustrate this, consider equation (2.2) in which we assume, without loss of generality, that $R_1 \leq R_2$. The quantity $a_1 - a_2 = R_2^2 - R_1^2$ is then the distance between the two poles, and the bipolar coordinates (ρ_1, ρ_2) must satisfy

$$\rho_1 + \rho_2 \geq a_1 - a_2 \qquad \text{and} \qquad |\rho_1 - \rho_2| \leq a_1 - a_2. \tag{2.4}$$

Equation (2.2) defines four lines in the (ρ_1, ρ_2) plane, only two of which possess segments in the region (2.4), shown in Figure 3. Table 1 lists the appropriate members from (2.2) that define the two loops of a Cartesian oval.

Table 1. The appropriate members from equations (2.2) defining the inner and outer loops of a Cartesian oval, assuming that $R_1, R_2 \neq 1$ and $R_1 < R_2$.

	Cartesian oval equations	
	inner loop	outer loop
$R_1 < 1$	$R_2\rho_1 + R_1\rho_2 = a_1 - a_2$	$R_2\rho_1 - R_1\rho_2 = a_1 - a_2$
$R_1 > 1$	$R_2\rho_1 - R_1\rho_2 = a_2 - a_1$	$R_2\rho_1 - R_1\rho_2 = a_1 - a_2$

2.2. GEOMETRICAL CONSTRUCTION

The Cartesian oval (2.3) admits the following geometrical construction [14], [32]: assuming $R_1 \leq R_2$, we consider two circular cones with axes perpendicular to the (x, y) plane—the vertices of these cones are at heights

$$z_1 = \frac{a_1}{a_1 - a_2} \qquad \text{and} \qquad z_2 = \frac{a_2}{a_1 - a_2} \tag{2.5}$$

above the points $(a_1, 0)$ and $(a_2, 0)$, and have half-angles

$$\psi_1 = \tan^{-1}\frac{a_1 - a_2}{R_2} \qquad \text{and} \qquad \psi_2 = \tan^{-1}\frac{a_1 - a_2}{R_1}. \tag{2.6}$$

Note that, since $z_1 : z_2 = a_1 : a_2$, the line through the vertices passes through the origin. The two cones intersect in a quartic space curve, and the Cartesian oval (2.3) is the projection of this curve onto the (x, y) plane. This can be seen by noting that a point at height z above the plane and distances ρ_1, ρ_2 from the cone axes lies on both cones if

$$\pm\tan\psi_1 = \frac{\rho_1}{z_1 - z} \qquad \text{and} \qquad \pm\tan\psi_2 = \frac{\rho_2}{z_2 - z}.$$

Eliminating z and substituting from (2.5) and (2.6) for z_1, z_2 and $\tan\psi_1$, $\tan\psi_2$ then results in the bipolar equation (2.2) for the projection of the intersection curve. The cases $R_1 = 1 \neq R_2$ or $R_1 \neq 1 = R_2$ defining a limaçon of Pascal correspond to configurations where the vertex of one cone lies on the other cone, inducing a singular point in the intersection.*

2.3. ENVELOPE METHODS

Since the Minkowski product of two circles can be regarded as a union of the scalings/rotations of one circle by each point of the other circle, its boundary amounts to the envelope of such a one-parameter family of circles. Let

$$f_1(\mathbf{z}) = (x - 1)^2 + y^2 - R_1^2 = 0 \tag{2.7}$$

---

* Cases with $R_1 = R_2$ should be considered as the limits $R_1 \rightarrow R_2$ of cases with distinct radii: in such cases, $|z_1|, |z_2| \rightarrow \infty$ and $\psi_1, \psi_2 \rightarrow 0$, i.e., the cones degenerate into cylinders.

(where $\mathbf{z} = x + iy$) be the implicit equation of $\mathcal{C}_1$, and let

$$\mathbf{z}_2(\theta) = 1 + R_2 \cos\theta + iR_2 \sin\theta \tag{2.8}$$

be a parameterization of $\mathcal{C}_2$. The scaling/rotation of $\mathcal{C}_1$ by each point of $\mathcal{C}_2$ then yields the family of circles

$$\begin{aligned}
h_1(\mathbf{z}, \theta) &= f_1\big(\mathbf{z} / \mathbf{z}_2(\theta)\big) \\
&= (x - 1 - R_2 \cos\theta)^2 + (y - R_2 \sin\theta)^2 - (R_2^2 + 2R_2 \cos\theta + 1)R_1^2 = 0,
\end{aligned}$$

whose envelope, obtained [2], [4] by eliminating θ among the equations

$$h_1 = \frac{\partial h_1}{\partial\theta} = 0,$$

is found to be the Cartesian oval

$$f_2(\mathbf{z}) = (x^2 + y^2 - 2x + a_1 a_2)^2 - 4R_1^2 R_2^2 (x^2 + y^2) = 0, \tag{2.9}$$

i.e., the boundary (2.3) of $\mathcal{C}_1 \otimes \mathcal{C}_2$. This method can, in principle, be extended to the Minkowski product of N disks. Suppose, for example, that

$$\mathbf{z}_3(\theta) = 1 + R_3 \cos\theta + iR_3 \sin\theta$$

defines a third circle $\mathcal{C}_3$. Then the one-parameter family of Cartesian ovals

$$\begin{aligned}
h_2(\mathbf{z}, \theta) &= f_2\big(\mathbf{z} / \mathbf{z}_3(\theta)\big) \\
&= [x^2 + y^2 - 2(1 + R_3 \cos\theta)x - 2R_3 \sin\theta\, y + (R_3^2 + 2R_3 \cos\theta + 1)a_1 a_2]^2 \\
&\quad - 4R_1^2 R_2^2 (R_3^2 + 2R_3 \cos\theta + 1)(x^2 + y^2) = 0
\end{aligned}$$

corresponds to the scaling/rotation of (2.9) by each point of $\mathcal{C}_3$. The boundary of the product $\mathcal{C}_1 \otimes \mathcal{C}_2 \otimes \mathcal{C}_3$ is thus (a subset of) the envelope of this family, obtained by eliminating θ among the equations

$$h_2 = \frac{\partial h_2}{\partial\theta} = 0.$$

Although this can be continued indefinitely, the method is of limited practical value. For $N \geq 3$, the resulting equations are very cumbersome, and offer no insight into the geometry of the Minkowski product. We shall see in Section 4 that the implicit equation of an N-circle product defines an irreducible algebraic curve comprising, in general, 2^{N-1} real loops. An explicit parameterization of the outermost loop, derived in Section 4 below, is a much more useful result.

2.4. Inversion in Circles

The Cartesian oval defined by equations (2.1), (2.2), or (2.3) has some remarkable symmetry properties under certain mappings of the complex plane.

DEFINITION 2.1. For a circle $\mathcal{C}$ with center $\mathbf{c}$ and radius R in the complex plane, the mappings $\mathbf{z} \to \mathbf{w}$ defined by

$$\mathbf{w} = \mathbf{c} \pm \frac{R^2}{|\mathbf{z} - \mathbf{c}|^2} (\mathbf{z} - \mathbf{c}) \tag{2.10}$$

are known as *inversions* with respect to $\mathcal{C}$. The $+$ and $-$ sign choices in (2.10) define, respectively, a "hyperbolic" and an "elliptic" inversion [30].

Geometrically, inversion is a one-to-one mapping of the interior of $\mathcal{C}$ onto its exterior,[*] and vice-versa. Any point $\mathbf{z}$ and its image $\mathbf{w}$ lie on a diametral line through the center $\mathbf{c}$, and their distances from $\mathbf{c}$ satisfy the relation

$$|\mathbf{z} - \mathbf{c}| \, |\mathbf{w} - \mathbf{c}| = R^2.$$

Note that $\mathbf{z}$ and $\mathbf{w}$ lie on the same side of $\mathbf{c}$ on the diametral line if we take the $+$ sign in (2.10), and on opposite sides if we take the $-$ sign.

Inversion, also known as a *transformation by reciprocal radii* or *reflection in a circle*, is clearly an "involutory"—i.e., self-inverse—mapping. Some well-known properties are as follows (see [3], [24], [25], [30] for details):

1. Lines passing through $\mathbf{c}$ are mapped into themselves.
2. Lines that do not pass through $\mathbf{c}$ map into circles through $\mathbf{c}$.
3. Circles through $\mathbf{c}$ map into lines that do not pass through $\mathbf{c}$.
4. Circles that do not pass through $\mathbf{c}$ map into other circles that do not pass through $\mathbf{c}$.
5. If $\tilde{\mathbf{p}}$ and $\tilde{\mathbf{q}}$ are the images of $\mathbf{p}$ and $\mathbf{q}$, then $\triangle \, \tilde{\mathbf{q}} \, \mathbf{c} \, \tilde{\mathbf{p}} \sim \triangle \, \mathbf{p} \, \mathbf{c} \, \mathbf{q}$.
6. Angles are preserved in magnitude, but reversed in sense.

Note that the two poles $a_1 = 1 - R_1^2$, $a_2 = 1 - R_2^2$ of the Cartesian oval introduced in Section 2.1 are the images of the origin under inversion in the circles $\mathcal{C}_1$, $\mathcal{C}_2$. Cartesian ovals exhibit some surprising symmetries under inversion:

PROPOSITION 2.1. *The Cartesian oval (2.3) maps onto[**] itself under an inversion in any of the circles defined by*

1. $\mathbf{c} = 0$ and $R^2 = a_1 a_2$,
2. $\mathbf{c} = a_1$ and $R^2 = a_1(R_2^2 - R_1^2)$,
3. $\mathbf{c} = a_2$ and $R^2 = a_2(R_1^2 - R_2^2)$.

Among the three poles 0, a_1, a_2 the one that is the center of inversion remains fixed, while the other two are swapped.

This can be readily verified by writing $\mathbf{z} = x + \mathrm{i}y$ and $\mathbf{w} = u + \mathrm{i}v$ in (2.10), and showing that (u, v) satisfies equation (2.3) if and only if (x, y) satisfies it. Note that

---

[*] Circumferential points are invariant, and the points $\mathbf{c}$ and ∞ are images of each other.
[**] Depending upon the values of R_1, R_2 and the chosen circle of inversion, the inner and outer loops may be individually mapped onto themselves, or onto each other.

the circles of inversion are *real*[*] circles—when $R^2 > 0$ we choose the $+$ sign in (2.10) and the radius is $\sqrt{R^2}$; and when $R^2 < 0$ we choose the $-$ sign and the radius is $\sqrt{-R^2}$. Exceptionally, the inversion (2.10) degenerates to the identity map if $R^2 = 0$ (and the Cartesian oval becomes a limaçon).

Curves that can be mapped onto themselves by inversion in a circle are known as *anallagmatic curves* [6]. Any circle that cuts the circle of inversion orthogonally is anallagmatic. Moreover, a family of circles, whose members all intersect the circle of inversion orthogonally, has an envelope curve that is anallagmatic [6]. This is a characteristic feature of the circles of inversion identified in Proposition 2.1—if we regard the Cartesian oval $\partial(\mathcal{C}_1 \otimes \mathcal{C}_2)$ as the envelope of the family of circles obtained by scaling/rotating $\mathcal{C}_1$ by each point of $\mathcal{C}_2$ (or vice-versa), then these scaled/rotated circles are all orthogonal to each of the three specified circles of inversion.

3. Minkowski Product of Two Disks

In computing the Minkowski product of circles $\mathcal{C}_1$, $\mathcal{C}_2$ with center 1 and radii R_1, R_2 it seems natural to use their polar representations $\mathbf{z}_1(\theta_1) = 1 + R_1 e^{i\theta_1}$, $\mathbf{z}_2(\theta_2) = 1 + R_2 e^{i\theta_2}$ with respect to the common center. However, we shall presently discover that different representations are advantageous in deriving a closed-form parameterization for the Minkowski product boundary.

3.1. IDENTIFICATION OF CORRESPONDING POINTS

Pairs of points on $\mathcal{C}_1$, $\mathcal{C}_2$ that contribute to the Minkowski product boundary $\partial(\mathcal{C}_1 \otimes \mathcal{C}_2)$ must have matched *logarithmic Gauss maps* [11]—i.e., for some non-zero real value k they must satisfy

$$\frac{\mathbf{z}_1'(\theta_1)}{\mathbf{z}_1(\theta_1)} = k \frac{\mathbf{z}_2'(\theta_2)}{\mathbf{z}_2(\theta_2)}. \tag{3.1}$$

Geometrically, this condition states that pairs of corresponding points on the two circles are identified by the fact that, at such points, *the angles between the tangent vectors and position vectors are equal modulo*[**] π. Consequently, the angles between the normal vectors and position vectors are likewise equal (modulo π). Since the position vectors pass through 0 and the normal vectors pass through 1, one can readily see that the angles α_1, α_2 subtended by the interval $[0, 1]$ at corresponding points $\mathbf{z}_1 \in \mathcal{C}_1$, $\mathbf{z}_2 \in \mathcal{C}_2$ of the circles must satisfy either $\alpha_1 = \alpha_2$ or $\alpha_1 = \pi - \alpha_2$, according to whether $\mathbf{z}_1$, $\mathbf{z}_2$ lie on the same side or opposite sides of the real axis, respectively.

We can deduce from these observations that corresponding points $\mathbf{z}_1$, $\mathbf{z}_2$ lie on a circle passing through 0 and 1. Figure 4 illustrates this for the case $R_1 < R_2 < 1$, with

---

[*] The sign choice in (2.10) can be omitted if we allow circles of inversion to have both real and imaginary radii, but we prefer to deal with real circles only.

[**] Equality modulo π is necessary, since k in (3.1) may be either positive or negative.
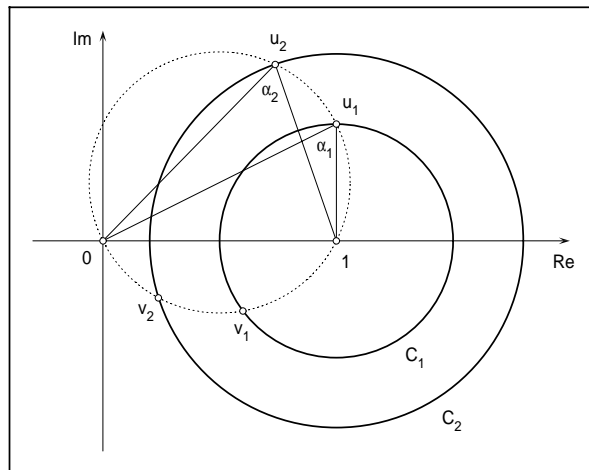
Figure 4. Pairs of corresponding points on the circles $\mathcal{C}_1$ and $\mathcal{C}_2$ are identified by the property that the angles α_1 and α_2 subtended by the interval $[0, 1]$ at such points satisfy either $\alpha_1 = \alpha_2$ or $\alpha_1 = \pi - \alpha_2$, according to whether the points lie on the same side or on opposite sides of the real axis, respectively. Such points therefore lie on a circle that passes through 0 and 1. Here, points above the real axis are labelled $\mathbf{u}_1$, $\mathbf{u}_2$ and those below are labelled $\mathbf{v}_1$, $\mathbf{v}_2$.
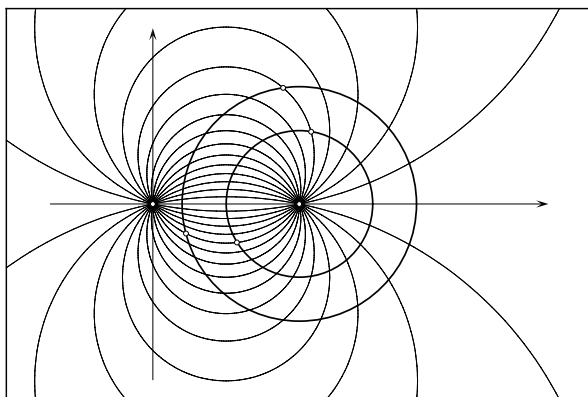
Figure 5. The coaxal system of circles with common points 0 and 1, and the operands $\mathcal{C}_1$, $\mathcal{C}_2$ with center 1 and radii R_1, R_2. Corresponding points, whose products may lie on $\partial(\mathcal{C}_1 \otimes \mathcal{C}_2)$, correspond to intersections of members of the coaxal system with $\mathcal{C}_1$ and $\mathcal{C}_2$. This generalizes to N operands $\mathcal{C}_1, ..., \mathcal{C}_N$.

points lying above and below the real axis labelled $\mathbf{u}_1$, $\mathbf{u}_2$ and $\mathbf{v}_1$, $\mathbf{v}_2$ respectively—the products $\mathbf{u}_1\mathbf{u}_2$ and $\mathbf{v}_1\mathbf{v}_2$ then yield points on the outer loop of the Cartesian oval, while $\mathbf{u}_1\mathbf{v}_2$ and $\mathbf{v}_1\mathbf{u}_2$ are points on the inner loop. By considering the family of coaxal circles with common points 0 and 1, we identify all pairs of corresponding points on $\mathcal{C}_1$, $\mathcal{C}_2$ (Figure 5).

Note that the characterization of corresponding points on C_1, C_2 as their intersections with the family of circles through 0 and 1 makes no reference to the radii R_1, R_2. Consequently, it is valid for *any* two circles, and it may also be generalized to identify corresponding N-tuples of points in the Minkowski product of N circles (an analytic proof will be given in Proposition 4.2 below).

3.2. ANGULAR PARAMETERIZATION

Condition (3.1) can be simplified to obtain the equation

$$\frac{\sin \theta_1}{R_1 + \cos \theta_1} = \frac{\sin \theta_2}{R_2 + \cos \theta_2}, \tag{3.2}$$

identifying corresponding points on the two circles. Setting $t = \tan(1/2)\theta_2$ gives the quadratic equation

$$(R_2 - 1) \sin \theta_1 \, t^2 - 2(R_1 + \cos \theta_1) \, t + (R_2 + 1) \sin \theta_1 = 0, \tag{3.3}$$

which may by solved to obtain θ_2 in terms of θ_1 as

$$\theta_2 = 2 \tan^{-1} \frac{R_1 + \cos \theta_1 \pm \sqrt{(R_1 + \cos \theta_1)^2 + a_2 \sin^2 \theta_1}}{(R_2 - 1) \sin \theta_1}, \tag{3.4}$$

If $R_2 \leq 1$, the discriminant of (3.3) is positive for all θ_1, and hence two values of θ_2 are associated with each θ_1. If $R_2 > 1$, however, θ_1 must be restricted to the domain over which the discriminant remains positive (since, outside this domain, the logarithmic Gauss map on the first circle cannot be matched to that of any point of the second circle).

The two loops of the Cartesian oval that bounds $C_1 \otimes C_2$ can, in principle, be parameterized in terms of the angle θ_1 by substituting from (3.4) into

$$\mathbf{z}_1(\theta_1) \, \mathbf{z}_2(\theta_2) = 1 + R_1 e^{i\theta_1} + R_2 e^{i\theta_2} + R_1 R_2 e^{i(\theta_1 + \theta_2)}. \tag{3.5}$$

Similarly, eliminating θ_1 and θ_2 among (3.2) and the equations

$$\begin{aligned} x &= 1 + R_1 \cos \theta_1 + R_2 \cos \theta_2 + R_1 R_2 \cos(\theta_1 + \theta_2), \\ y &= 1 + R_1 \sin \theta_1 + R_2 \sin \theta_2 + R_1 R_2 \sin(\theta_1 + \theta_2), \end{aligned}$$

we can recover the implicit equation (2.3) of the Cartesian oval. However, this is clearly a very cumbersome approach—especially if our goal is to achieve a generalization to the Minkowski product of N disks.

The complication stems from our insistence on parameterizing the circle operands C_1, C_2 in terms of angular positions about their common center 1. Based on geometrical insight, we now show that a more tractable formulation (extensible to the case of N disks) may be based upon a special "coordinated" polar parameterization of the circle operands, that automatically identifies corresponding points with matched logarithmic Gauss maps.
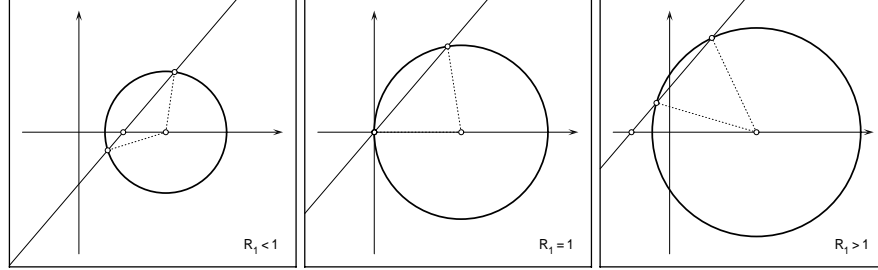
Figure 6. Intersections of the circle $\mathcal{C}_1$, with center 1 and radius R_1, and the line $\mathcal{L}_1$ through the point $a_1 = 1 - R_1^2$ and at angle φ with the real axis, in the cases $R_1 < 1$, $R_1 = 1$, $R_1 > 1$. In each case, the intersections can be expressed as $1 + R_1 e^{i\theta_1}$, where the polar angle θ_1 satisfies $\tan \varphi = \sin \theta_1 / (R_1 + \cos \theta_1)$.

LEMMA 3.1. *Let $\mathcal{C}_1$ and $\mathcal{C}_2$ be circles with center 1 and radii R_1 and R_2, and let $\mathcal{L}_1$ and $\mathcal{L}_2$ be parallel lines through the points $a_1 = 1 - R_1^2$ and $a_2 = 1 - R_2^2$ on the real axis. Then the intersections of $\mathcal{L}_1$ with $\mathcal{C}_1$ and $\mathcal{L}_2$ with $\mathcal{C}_2$ identify pairs of points $\mathbf{z}_1 \in \mathcal{C}_1$, $\mathbf{z}_2 \in \mathcal{C}_2$ such that $\mathbf{z}_1 \mathbf{z}_2$ may lie on $\partial(\mathcal{C}_1 \otimes \mathcal{C}_2)$.*

Proof. Let $\mathcal{L}_1$ be the line through $a_1 = 1 - R_1^2$ at angle φ with the real axis, where we take $-\pi/2 < \varphi \le +\pi/2$. If $R_1 < 1$, the line $\mathcal{L}_1$ has two intersections with the circle $\mathcal{C}_1$ (one above and one below the real axis) for any φ. If $R_1 > 1$, however, $\mathcal{L}_1$ intersects $\mathcal{C}_1$ only when $-\sin^{-1}(1/R_1) \le \varphi \le +\sin^{-1}(1/R_1)$—the intersections are both above or both below the real axis. In the degenerate case $R_1 = 1$, there is one intersection at the origin and another above or below the axis. Figure 6 illustrates the geometry of these configurations.

Now suppose $R_1 < 1$, and let the intersections of $\mathcal{L}_1$ and $\mathcal{C}_1$ be specified in polar form as $1 + R_1 e^{i\theta_1}$. Consider the right triangle with vertices $a_1 = 1 - R_1^2$ on the real axis, the point $1 + R_1 e^{i\theta_1}$ on $\mathcal{C}_1$, and the projection $1 + R_1 \cos \theta_1$ of the latter onto the real axis. This triangle has angle φ at a_1, and simple trigonometric arguments applied to Figure 6 reveal that, for the intersection above the real axis ($0 < \theta_1 < +\pi$), we have

$$\tan \varphi = \frac{R_1 \sin \theta_1}{R_1 \cos \theta_1 + R_1^2} = \frac{\sin \theta_1}{R_1 + \cos \theta_1}, \tag{3.6}$$

while for the intersection below the real axis ($-\pi < \theta_1 < 0$),

$$\tan \varphi = \frac{R_1 \sin(\pi + \theta_1)}{R_1 \cos(\pi + \theta_1) - R_1^2} = \frac{\sin \theta_1}{R_1 + \cos \theta_1}.$$

Thus, the two intersections are characterized by a common value for the ratio $\sin \theta_1 / (R_1 + \cos \theta_1)$, equal to $\tan \varphi$.

When $R_1 > 1$, one can similarly see from Figure 6 that both intersections, expressed in the form $1 + R_1 e^{i\theta_1}$, satisfy (3.6) regardless of whether they are above or below the real axis. Finally, when $R_1 = 1$, the intersection distinct from 0

clearly satisfies relation (3.6) with $R_1 = 1$. We may also consider the intersection at the origin to satisfy this relation, in the sense that right hand side of (3.6) is indeterminate when $R_1 = 1$ and $\theta_1 = \pm\pi$, indicating that 0 is an intersection of $\mathcal{L}_1$ and $\mathcal{C}_1$ for *any* orientation φ of the line.

Now exactly analogous arguments hold for the intersections $1 + e^{i\theta_2}$ of $\mathcal{L}_2$ and $\mathcal{C}_2$. Thus, if $\mathcal{L}_1$ and $\mathcal{L}_2$ are parallel (i.e., make the same angle φ with the real axis) we must have

$$\tan\varphi = \frac{\sin\theta_1}{R_1 + \cos\theta_1} = \frac{\sin\theta_2}{R_2 + \cos\theta_2}. \tag{3.7}$$

Hence, the intersections of $\mathcal{L}_1$ with $\mathcal{C}_1$ and $\mathcal{L}_2$ with $\mathcal{C}_2$ satisfy the condition (3.2) characterizing matched logarithmic Gauss maps on the two circles, and their products may therefore lie on $\partial(\mathcal{C}_1 \otimes \mathcal{C}_2)$. □

From Lemma 3.1 we see that, to compute the Minkowski product $\mathcal{C}_1 \otimes \mathcal{C}_2$, it is advantageous to employ polar forms of the circles $\mathcal{C}_1, \mathcal{C}_2$ with respect to the points a_1, a_2 (rather than their common center 1) as poles. Writing

$$\mathbf{z}_k(\varphi) = a_k + \rho_k(\varphi)\, e^{i\varphi} \tag{3.8}$$

with $k = 1, 2$ for $\mathcal{C}_1, \mathcal{C}_2$, a straightforward calculation yields

$$\rho_k(\varphi) = R_k^2 \cos\varphi + \sigma_k R_k \sqrt{1 - R_k^2 \sin^2\varphi}, \qquad \sigma_k = \pm 1 \tag{3.9}$$

for the polar distance in terms of the polar angle φ. When $R_k \leq 1$, expression (3.9) yields one positive and one negative value for each φ, the negative value corresponding to $\rho_k(\pi - \varphi)$. When $R_k > 1$, on the other hand, we have two positive values if $|\sin\varphi| \leq 1/R_k$, and ρ_k is undefined outside this domain.

Henceforth we shall assume, without loss of generality, that $R_1 \leq R_2$. By Lemma 3.1, expressions (3.8)–(3.9) with $k = 1, 2$ define parameterizations of the circles $\mathcal{C}_1, \mathcal{C}_2$ such that, for each φ, the point $\mathbf{z}(\varphi) = \mathbf{z}_1(\varphi)\mathbf{z}_2(\varphi)$ may lie on the Minkowski product boundary. Thus we may write

$$\mathbf{z}(\varphi) = [a_1 + \rho_1(\varphi)\, e^{i\varphi}]\,[a_2 + \rho_2(\varphi)\, e^{i\varphi}] \tag{3.10}$$

as a parameterization of (a superset of) $\partial(\mathcal{C}_1 \otimes \mathcal{C}_2)$. The interpretation of this expression requires careful consideration of the combinations of signs chosen from (3.9) and the appropriate domain for φ, as follows.

The Minkowski product of two circles $\mathcal{C}_1, \mathcal{C}_2$ is the area between the two loops of a Cartesian oval; the Minkowski product of the disks $\mathcal{D}_1, \mathcal{D}_2$ bounded by these circles is the area within the *outer* loop of the Cartesian oval [12]. When $R_2 \leq 1$, it is not necessary to invoke all four sign combinations implied by (3.9) in expression (3.10): with $-\pi \leq \varphi \leq +\pi$, the outer loop is completely generated by either the ++ or −− choice, and the inner loop⋆ by either +− or −+. When $R_2 > 1$, however, all four sign combinations are necessary—with $-\varphi_{\max} \leq \varphi \leq +\varphi_{\max}$, where

$$\varphi_{\max} = \sin^{-1}(1/R_2),$$

⋆ Note that, in the case $R_2 = 1 > R_1$, the inner and outer loops pinch together to form a limaçon of Pascal, while for $R_2 = R_1 = 1$ the inner loop vanishes to produce a cardioid.

the $++$ and $+-$ choices generate complementary segments of the outer loop, while $--$ and $-+$ yield complementary segments of the inner loop. We may summarize these observations as follows:

PROPOSITION 3.1. *Let $\mathcal{D}_1$ and $\mathcal{D}_2$ be two circular disks in the complex plane with center 1 and radii R_1, R_2 such that $R_1 \leq R_2$. Then the boundary $\partial(\mathcal{D}_1 \otimes \mathcal{D}_2)$ of their Minkowski product is either*

1. *the locus defined by (3.10) with $\sigma_1 = \sigma_2 = 1$ in (3.9), for $-\pi \leq \varphi \leq +\pi$, when $R_2 \leq 1$, or*
2. *the union of the loci defined by (3.10) with $\sigma_1 = \sigma_2 = 1$ and $\sigma_1 = -\sigma_2 = 1$ in (3.9), for $-\varphi_{\max} \leq \varphi \leq +\varphi_{\max}$, when $R_2 > 1$.*

3.3. GEOMETRICAL DERIVATION OF BIPOLAR EQUATION

The bipolar equation of the Cartesian oval bounding the Minkowski product of two circles can be derived by elegant geometrical arguments, based upon *Ptolemy's theorem* relating the sides and diagonals of a quadrilateral [15], [24]. The theorem states that, for any quadrilateral $ABCD$, we have

$$AB \cdot CD + BC \cdot DA \geq AC \cdot BD,$$

where the equality holds only if $ABCD$ is a *cyclic* quadrilateral.

Consider two circles $\mathcal{C}_1$, $\mathcal{C}_2$ with center 1 and radii R_1, R_2. For simplicity, we focus on the case $R_1 < R_2 < 1$ and choose the points 0 and a_1 on the real axis as poles—the appropriate equations from (2.1) describing the inner and outer loops of the Cartesian oval are then

$$R_1 \rho_0 + \rho_1 = a_1 R_2 \qquad \text{and} \qquad R_1 \rho_0 - \rho_1 = -a_1 R_2.$$

The argument can be readily adapted to other configurations. As in Figure 4, a circle $\mathcal{C}$ through 0 and 1 is constructed with center on the line $\text{Re}(\mathbf{z}) = 1/2$, intersecting $\mathcal{C}_1$ and $\mathcal{C}_2$ in pairs of corresponding points $\mathbf{u}_1$, $\mathbf{u}_2$ (above the real axis) and $\mathbf{v}_1$, $\mathbf{v}_2$ (below the real axis), such that the products $\mathbf{u}_1\mathbf{u}_2$ and $\mathbf{v}_1\mathbf{v}_2$ yield distinct points on the outer loop of the Cartesian oval $\partial(\mathcal{C}_1 \otimes \mathcal{C}_2)$, while $\mathbf{u}_1\mathbf{v}_2$ and $\mathbf{v}_1\mathbf{u}_2$ yield distinct points on the inner loop.

Consider first the point $\mathbf{c} = \mathbf{u}_1\mathbf{u}_2$ on the outer loop, and let $\rho_0 = |\mathbf{c}| = |\mathbf{u}_1| \, |\mathbf{u}_2|$ and $\rho_1 = |\mathbf{c} - a_1|$ be its distances from the origin and point a_1 on the real axis. We consider the quadrilateral inscribed in $\mathcal{C}$ with 0, $\mathbf{u}_2$, 1, $\mathbf{v}_1$ as the vertices A, B, C, D. Then $AB = |\mathbf{u}_2|$, $CD = R_1$, $BC = R_2$, $DA = |\mathbf{v}_1|$, $AC = 1$, $BD = |\mathbf{u}_2 - \mathbf{v}_1|$, and by Ptolemy's theorem we have

$$R_1 |\mathbf{u}_2| + R_2 |\mathbf{v}_1| = |\mathbf{u}_2 - \mathbf{v}_1|. \tag{3.11}$$

Multiplying both sides by $|\mathbf{u}_1|$ and setting $|\mathbf{u}_1| \, |\mathbf{u}_2| = \rho_0$ then gives

$$R_1 \rho_0 + R_2 |\mathbf{u}_1| \, |\mathbf{v}_1| = |\mathbf{u}_2 - \mathbf{v}_1| \, |\mathbf{u}_1|. \tag{3.12}$$

Now let $\mathcal{C}'$ be the image of $\mathcal{C}$ under a reflection in the real axis, intersecting the circles $\mathcal{C}_1$ and $\mathcal{C}_2$ in the conjugates $\bar{\mathbf{u}}_1$, $\bar{\mathbf{v}}_1$ and $\bar{\mathbf{u}}_2$, $\bar{\mathbf{v}}_2$ of $\mathbf{u}_1$, $\mathbf{v}_1$ and $\mathbf{u}_2$, $\mathbf{v}_2$. Then $\mathbf{u}_1$ and $\bar{\mathbf{v}}_1$ lie on a line through the origin, and the product $|\mathbf{u}_1|\,|\bar{\mathbf{v}}_1|$ is the *power** of the origin with respect to the circle $\mathcal{C}_1$, with value $1 - R_1^2 = a_1$. Thus, since $|\bar{\mathbf{v}}_1| = |\mathbf{v}_1|$, we can substitute $|\mathbf{u}_1|\,|\mathbf{v}_1| = a_1$ in (3.12).

Consider also the triangle with vertices 0, $\mathbf{v}_1$, $\mathbf{u}_2$. Multiplying this triangle by the complex value $\mathbf{u}_1$ maps it into the triangle with vertices 0, a_1, $\mathbf{c}$. The mapping of 0 to 0 and of $\mathbf{u}_2$ to $\mathbf{c} = \mathbf{u}_1\mathbf{u}_2$ is obvious: to see that $\mathbf{u}_1\mathbf{v}_1 = a_1$, we use the result $|\mathbf{u}_1|\,|\mathbf{v}_1| = a_1$, proved above, and that $\arg(\mathbf{v}_1) = -\arg(\bar{\mathbf{v}}_1) = -\arg(\mathbf{u}_1)$, since $\mathbf{u}_1$ and $\bar{\mathbf{v}}_1$ lie on a line through the origin. By similarity of the two triangles, we have

$$\frac{|\mathbf{c} - a_1|}{|\mathbf{c}|} = \frac{|\mathbf{u}_2 - \mathbf{v}_1|}{|\mathbf{u}_2|},$$

and thus $|\mathbf{u}_2 - \mathbf{v}_1|\,|\mathbf{u}_1| = \rho_1$ since $\rho_1 = |\mathbf{c} - a_1|$ and $|\mathbf{c}| = |\mathbf{u}_1|\,|\mathbf{u}_2|$. Substituting this and the result $|\mathbf{u}_1|\,|\mathbf{v}_1| = a_1$ into (3.12) and re-arranging, we obtain

$$R_1\rho_0 - \rho_1 = -a_1 R_2$$

as the equation of the outer loop. The same result is obtained if we choose 0, $\mathbf{v}_2$, 1, $\mathbf{u}_1$ as A, B, C, D and apply similar arguments to $\mathbf{c} = \mathbf{v}_1\mathbf{v}_2$.

Consider now the point $\mathbf{c} = \mathbf{u}_1\mathbf{v}_2$ on the inner loop. Applying Ptolemy's theorem to the quadrilateral with vertices 0, $\mathbf{v}_2$, $\mathbf{v}_1$, 1 we obtain

$$R_1\,|\mathbf{v}_2| + |\mathbf{v}_1 - \mathbf{v}_2| = R_2\,|\mathbf{v}_1|.$$

Multiplying both sides by $|\mathbf{u}_1|$ and setting $|\mathbf{u}_1|\,|\mathbf{v}_2| = \rho_0$ then gives

$$R_1\rho_0 + |\mathbf{u}_1|\,|\mathbf{v}_1 - \mathbf{v}_2| = a_1 R_2$$

where we use the result $|\mathbf{u}_1|\,|\mathbf{v}_1| = a_1$, derived above, that also holds in this case. Finally, to interpret the quantity $|\mathbf{u}_1|\,|\mathbf{v}_1 - \mathbf{v}_2|$, we consider the triangle with vertices 0, $\mathbf{v}_1$, $\mathbf{v}_2$. Multiplying this triangle by $\mathbf{u}_1$ maps it to the triangle with vertices 0, a_1, $\mathbf{c}$. The mapping of 0 to 0 and of $\mathbf{v}_2$ to $\mathbf{c} = \mathbf{u}_1\mathbf{v}_2$ is obvious; and the result $\mathbf{u}_1\mathbf{v}_1 = a_1$, proved above, also holds in the present case. Thus, by similarity of these triangles, we have

$$\frac{|\mathbf{c} - a_1|}{|\mathbf{c}|} = \frac{|\mathbf{v}_1 - \mathbf{v}_2|}{|\mathbf{v}_2|},$$

and hence $|\mathbf{u}_1|\,|\mathbf{v}_1 - \mathbf{v}_2| = \rho_1$, since $\rho_1 = |\mathbf{c} - a_1|$ and $|\mathbf{c}| = |\mathbf{u}_1|\,|\mathbf{v}_2|$. Thereby we arrive at the equation of the inner loop,

$$R_1\rho_0 + \rho_1 = a_1 R_2.$$

---

* Recall [25] that the power of a point $\mathbf{p}$ with respect to a circle $\mathcal{C}$ is the product of the distances from $\mathbf{p}$ to the two points of intersection of $\mathcal{C}$ with any line through $\mathbf{p}$.

The same result will be obtained by choosing the quadrilateral with vertices 0, $\mathbf{u}_2$, $\mathbf{u}_1$, 1 and applying similar arguments to the point $\mathbf{c} = \mathbf{v}_1 \mathbf{u}_2$.

4. Minkowski Product of N Disks

The method used in Section 3.2 to compute the boundary of the Minkowski product of two disks is motivated by the fact that, as we shall now see, this approach admits direct generalization to the case of N disks. As usual, we assume that the disks all have center 1, and their radii satisfy $R_1 \leq \cdots \leq R_N$.

LEMMA 4.1. *Let* $\mathcal{C}_1, \ldots, \mathcal{C}_N$ *be circles with center* 1 *and radii* $R_1, \ldots, R_N$, *and let* $\mathcal{L}_1, \ldots, \mathcal{L}_N$ *be parallel lines through points* $a_1 = 1 - R_1^2, \ldots, a_N = 1 - R_N^2$ *on the real axis. Then for* $k = 1, \ldots, N$ *the intersections of* $\mathcal{L}_k$ *with* $\mathcal{C}_k$ *identify points* $\mathbf{z}_k \in \mathcal{C}_k$ *such that the products* $\mathbf{z}_1 \cdots \mathbf{z}_N$ *may lie on* $\partial(\mathcal{C}_1 \otimes \cdots \otimes \mathcal{C}_N)$.

Proof. The case $N = 2$ of this result, established in Lemma 3.1, arose from the identification of pairs of points $\mathbf{z}_1$, $\mathbf{z}_2$ with matched logarithmic Gauss maps on the two circles, as expressed by condition (3.2). The Minkowski product boundary is generated by the products $\mathbf{z} = \mathbf{z}_1 \mathbf{z}_2$ of such points. Furthermore, the logarithmic Gauss map of the Minkowski product boundary at the point $\mathbf{z}$ is matched to that of the circles at the points $\mathbf{z}_1$, $\mathbf{z}_2$ generating it [11].

By virtue of this "preservation of logarithmic Gauss map" property, we can argue by induction that we need not proceed sequentially—introducing one operand at a time—when computing the Minkowski product of N disks. Instead, we can deduce an *a priori* necessary condition for the product of N points $\mathbf{z}_k(\theta_k) = 1 + R_k \mathrm{e}^{\mathrm{i}\theta_k}$, $k = 1, \ldots, N$ to belong to $\partial(\mathcal{C}_1 \otimes \cdots \otimes \mathcal{C}_N)$ as the obvious generalization

$$\tan \varphi = \frac{\sin \theta_1}{R_1 + \cos \theta_1} = \cdots = \frac{\sin \theta_N}{R_N + \cos \theta_N} \tag{4.1}$$

of (3.7). Geometrically, φ is the common inclination angle of the parallel lines $\mathcal{L}_1, \ldots, \mathcal{L}_N$ with the real axis, and for $k = 1, \ldots, N$ the two solutions θ_k to (4.1) identify the intersections of the line $\mathcal{L}_k$ and circle $\mathcal{C}_k$.   □

Lemmas 3.1 and 4.1 can also be proved by geometrical arguments, as follows. A circle $\mathcal{C}$ among the coaxal system with common points 0 and 1 intersects the family of circles $\mathcal{C}_1, \mathcal{C}_2, \ldots$ with center 1 and different radii $R_1, R_2, \ldots$ in pairs of points that define parallel chords (since, by symmetry, these chords must be orthogonal to the line joining 1 and the center of $\mathcal{C}$). One can easily show that these chords cut the real axis in the points $a_1, a_2, \ldots$

Note that (3.7), and its generalization (4.1), can be solved to obtain

$$\theta_k = \varphi + \sin^{-1}(R_k \sin \varphi)$$
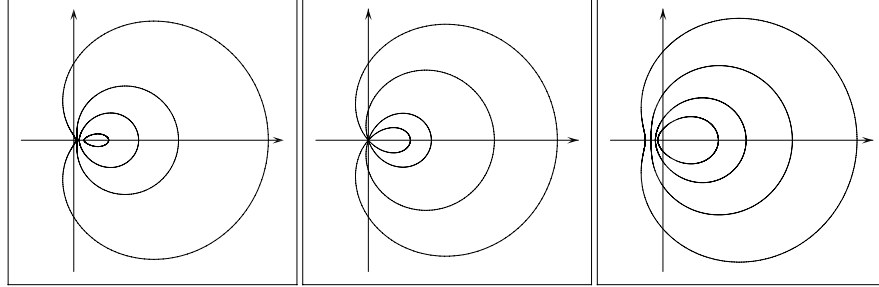
Figure 7. Examples of the curves defined by (4.2) with $N = 3$ and the choices 0.3, 0.5, 0.9 (left), 0.2, 0.5, 1.0 (center), and 0.2, 0.4, 1.2 (right) for R_1, R_2, R_3.

for the angular position on each circle $\mathcal{C}_k$, in terms of the common angle φ. By the same reasoning as in the case $N = 2$, we may now write

$$\mathbf{z}(\varphi) = \prod_{k=1}^{N} [a_k + \rho_k(\varphi) \, \mathrm{e}^{\mathrm{i}\varphi}] \tag{4.2}$$

as an explicit parameterization of (a superset of) $\partial(\mathcal{C}_1 \otimes \cdots \otimes \mathcal{C}_N)$. Assuming that $R_1 \leq \cdots \leq R_N$, the domain of expression (4.2) is $-\pi \leq \varphi \leq +\pi$ when $R_N \leq 1$, and $-\varphi_{\max} \leq \varphi \leq +\varphi_{\max}$ when $R_N > 1$, where

$$\varphi_{\max} = \sin^{-1}(1/R_N).$$

Allowing for all possible sign choices $\sigma_k = \pm 1$ for $k = 1, ..., N$ in (3.9), the curve defined by (4.2) comprises, in general, 2^{N-1} real loops. When $R_N \leq 1$, it suffices to fix $\sigma_1 = +1$ and vary the other signs to generate all 2^{N-1} loops: the outermost loop, in particular, corresponds to $\sigma_1 = \cdots = \sigma_N = 1$. If $R_N > 1$, however, all 2^N sign combinations are required—with $-\varphi_{\max} \leq \varphi \leq +\varphi_{\max}$, exercising the two choices $\sigma_r = \pm 1$ and fixing σ_k for all $k \neq r$ generates two complementary segments of a single loop (the outermost loop is defined by $\sigma_1 = \cdots = \sigma_{N-1} = 1$ and $\sigma_N = \pm 1$).

Figures 7 and 8 show examples of the curves defined by (4.2) with $N = 3$ and $N = 4$. The generic case has 2^{N-1} loops, although degenerate (singular) loci occur if any of $R_1, ..., R_N$ are coincident or equal to unity—these are generalizations of the limaçon and cardioid (see Section 5). A noteworthy difference between these curves and Cartesian ovals is that, for $N \geq 3$, the outermost loop of (4.2) may self-intersect (as seen in Figure 8). Thus, to obtain a faithful parameterization of $\partial(\mathcal{C}_1 \otimes \cdots \otimes \mathcal{C}_N)$, it is necessary to determine the φ values corresponding to the self-intersection, and restrict the domain $-\pi \leq \varphi \leq +\pi$ or $-\varphi_{\max} \leq \varphi \leq +\varphi_{\max}$ so as to exclude the portion of this loop lying *inside* the Minkowski product. We now generalize Proposition 3.1 as follows:

PROPOSITION 4.1. *Let $\mathcal{D}_1, ..., \mathcal{D}_N$ be N circular disks in the complex plane with center 1 and radii $R_1, ..., R_N$ such that $R_1 \leq \cdots \leq R_N$. Then the boundary $\partial(\mathcal{D}_1 \otimes \cdots \otimes \mathcal{D}_N)$ of their Minkowski product is (a subset of) either*
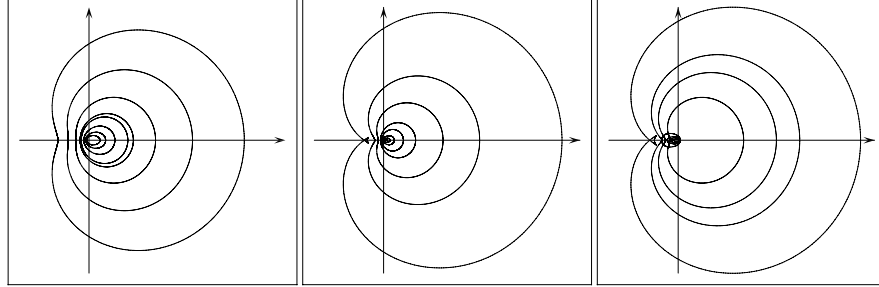
Figure 8.   Examples of the curves defined by (4.2) with $N = 4$ and $R_1, ..., R_4 = 0.2, 0.4, 0.6,$ 1.5 (left); 0.3, 0.5, 0.8, 1.2 (center); and 0.2, 0.3, 1.2, 1.3 (right).

1. *the locus defined by (4.2) with* $\sigma_1 = \cdots = \sigma_N = 1$ *in (3.9), for* $-\pi \leq \varphi \leq +\pi$, *when* $R_N \leq 1$, *or*

2. *the union of the loci defined by (4.2) with* $\sigma_1 = \cdots = \sigma_N = 1$ *and* $\sigma_1 = \cdots = -\sigma_N = 1$ *in (3.9), for* $-\varphi_{\max} \leq \varphi \leq +\varphi_{\max}$, *when* $R_N > 1$.

The qualification "a subset of" reflects a possible need to trim the outermost loop of (4.2) at values of φ (if any) corresponding to its self-intersection. With the appropriate $\sigma_1, ..., \sigma_N$ these can be identified as distinct φ values that give the same real part and vanishing imaginary part in (4.2).

We conclude this section by demonstrating the equivalence of the methods used to identify corresponding points in Section 3.1 and in Lemmas 3.1 and 4.1. These lemmas employ a family of parallel lines $\mathcal{L}_k$ through the points $a_k = 1 - R_k^2$ to construct coordinated polar representations for the circles $\mathcal{C}_1, ..., \mathcal{C}_N$—a closed-form parameterization for $\partial(\mathcal{C}_1 \otimes \cdots \otimes \mathcal{C}_N)$ is then derived, in terms of the common inclination angle φ of the lines. By inversion of each line $\mathcal{L}_k$ in the corresponding circle $\mathcal{C}_k$, we can show that this approach is equivalent to establishing correspondence by the intersections of $\mathcal{C}_1, ..., \mathcal{C}_N$ with members of the coaxal system of circles that pass through 0 and 1.

PROPOSITION 4.2. *Let* $\mathcal{C}_1, ..., \mathcal{C}_N$ *be circles with center* 1 *and radii* $R_1, ..., R_N$, *whose Minkowski product we wish to compute. Further, let* $\mathcal{C}(\varphi)$ *be the system of coaxal circles with common points* 0 *and* 1, *parameterized such that* $\mathcal{C}(\varphi)$ *has center* $\mathbf{c} = (1/2)(1 + \mathrm{i} \cot \varphi)$ *and radius* $R = (1/2)|\csc \varphi|$ *for* $-\pi/2 \leq \varphi \leq +\pi/2$. *Then, for each* φ, *the intersections* $\mathcal{C}(\varphi) \cap \mathcal{C}_k$ *identify sets of points* $\mathbf{z}_k \in \mathcal{C}_k$, $k = 1, ..., N$ *such that the product* $\mathbf{z}_1 \cdots \mathbf{z}_N$ *may lie on* $\partial(\mathcal{C}_1 \otimes \cdots \otimes \mathcal{C}_N)$.

Proof. Consider the line $\mathcal{L}_k$ through $a_k = 1 - R_k^2$ at angle φ to the real axis. From Section 2.4 we know that its image under inversion in $\mathcal{C}_k$ is a circle through 1

(the center of inversion), and the point a_k is mapped to 0. Furthermore, the two intersections of $\mathcal{L}_k$ with $\mathcal{C}_k$, given by $1 + R_k e^{i\theta_k}$ where θ_k satisfies[*]

$$\tan \varphi = \frac{\sin \theta_k}{R_k + \cos \theta_k}, \tag{4.3}$$

are invariant under inversion in $\mathcal{C}_k$. Hence, the image of $\mathcal{L}_k$ under inversion in $\mathcal{C}_k$ is a circle $\mathcal{C}(\varphi)$ passing through these two intersections points, dependent on φ, and the fixed points 0 and 1. One can verify that $\mathcal{C}(\varphi)$ has the equation

$$\left(x - \frac{1}{2}\right)^2 + \left(y - \frac{R_k + \cos \theta_k}{2 \sin \theta_k}\right)^2 - \left(\frac{R_k + \cos \theta_k}{2 \sin \theta_k}\right)^2 - \frac{1}{4} = 0.$$

Note that this depends only on the ratio $(R_k + \cos \theta_k) / \sin \theta_k$ which, by virtue of equation (4.1), has the same value $\cot \varphi$ for each k. Hence, for $k = 1, \dots, N$ the lines $\mathcal{L}_k$ are all mapped by inversion in the corresponding circles $\mathcal{C}_k$ into the *same* circle $\mathcal{C}(\varphi)$, given by

$$\left(x - \frac{1}{2}\right)^2 + \left(y - \frac{1}{2} \cot \varphi\right)^2 - \frac{1}{4} \csc^2 \varphi = 0 \tag{4.4}$$

(where we set $(R_k + \cos \theta_k) / \sin \theta_k = \cot \varphi$). For $-\pi/2 \le \varphi \le +\pi/2$, equation (4.4) defines a coaxal system of circles with common points 0, 1 and radical axis $x = 1/2$. Each member $\mathcal{C}(\varphi)$ of this system cuts the operands $\mathcal{C}_1, \dots, \mathcal{C}_N$ in corresponding points $\mathbf{z}_k = 1 + R_k e^{i\theta_k}$, $k = 1, \dots, N$ satisfying the necessary condition (4.1) for the product $\mathbf{z}_1 \cdots \mathbf{z}_N$ to lie on $\partial(\mathcal{C}_1 \otimes \cdots \otimes \mathcal{C}_N)$. $\qquad \square$

5. N-th Minkowski power of a disk

As a special instance of the Minkowski product of N disks, consider the case where the operands are identical, i.e., we are interested in the N-th *Minkowski power* of a single disk. Now let $\mathcal{C}$ be the circle $\mathbf{z}(\theta) = 1 + R e^{i\theta}$ for $0 \le \theta < 2\pi$. In computing the Minkowski power $\otimes^N \mathcal{C}$, it is obvious that the condition of matched logarithmic Gauss maps is satisfied when we choose the *same* point on each of the N copies of $\mathcal{C}$, as an N-tuple of corresponding points. Hence, we may expect the locus defined by

$$\mathbf{z}^N(\theta) = [1 + R e^{i\theta}]^N = \sum_{k=0}^{N} \binom{N}{k} R^k e^{ik\theta}, \qquad 0 \le \theta < 2\pi \tag{5.1}$$

to contribute to the boundary $\partial(\otimes^N \mathcal{C})$ of the N-th Minkowski power. However, for each φ between $-\sin^{-1}(1/R)$ and $+\sin^{-1}(1/R)$, the condition

$$\tan \varphi = \frac{\sin \theta}{R + \cos \theta}$$

[*] We assume that $-\varphi_{\max} \le \varphi \le +\varphi_{\max}$, where $\varphi_{\max} = \sin^{-1} 1/R_k$ if $R_k > 1$.
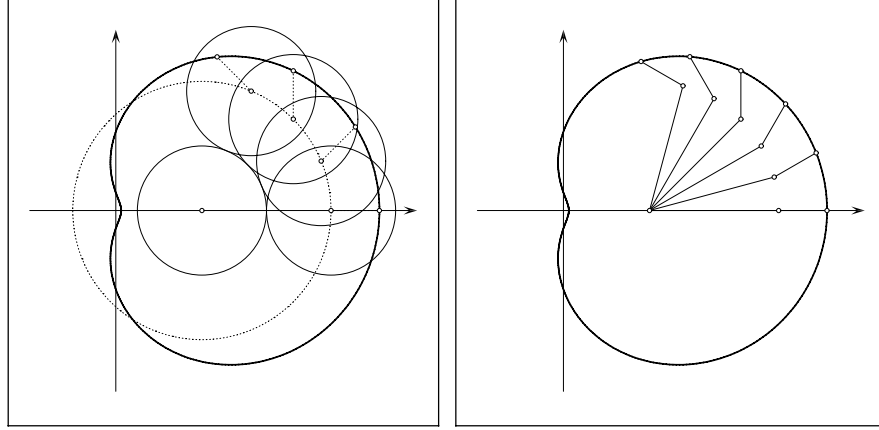
Figure 9. Generation of the limaçon of Pascal as a trochoid by: rolling motion of a circle of radius R on a fixed circle of radius R (left), and a two-bar linkage with links of length $2R$ and R^2 and angular velocities in the ratio 1:2 (right).

identifies a second *distinct* corresponding point θ' for any chosen point θ, such that products of the form $\mathbf{z}^{N-r}(\theta')\,\mathbf{z}^r(\theta)$ for $0 \le r \le N$ may also contribute to $\partial(\otimes^N \mathcal{C})$. In general, such products define a number of closed loops, among which (5.1) is the outermost.[⋆] Henceforth, we shall focus on the locus defined by expression (5.1), since (a subset of) this locus defines the boundary of the N-th Minkowski power of the circular disk $\mathcal{D}$ bounded by $\mathcal{C}$.

For $N = 2$, the curve (5.1) is a limaçon of Pascal, which may be interpreted kinematically as the trajectory of a point carried by a circle that rolls on a fixed base circle of equal radius—an example[⋆⋆] of *trochoidal motion* (in the present instance, the point that traces the limaçon is at distance R^2 from the center of the rolling circle). From the form

$$\mathbf{z}^2(\theta) = 1 + 2Re^{i\theta} + R^2 e^{2i\theta}, \qquad 0 \le \theta \le 2\pi \tag{5.2}$$

we see that the limaçon can also be generated by a two-bar linkage: the first bar has length $2R$ and rotates with angular velocity 1 about the point 1 on the real axis, while the second bar has length R^2 and rotates with angular velocity 2 about the end point of the first bar[‡] (see Figure 9). When $R = 1$, we obtain a limaçon with a cusp—namely, a cardioid.

Now for arbitrary $N > 2$, expanding (5.1) gives

$$\mathbf{z}^N(\theta) = 1 + NRe^{i\theta} + \binom{N}{2}R^2 e^{i2\theta} + \cdots + R^N e^{iN\theta}, \qquad 0 \le \theta \le 2\pi. \tag{5.3}$$

[⋆] When $N = 2$, one can easily verify that $\mathbf{z}(\theta')\,\mathbf{z}(\theta) = 1 - R^2$ for all φ—i.e., the inner loop collapses to a single point on the real axis, which is a singular point of the locus (5.1).

[⋆⋆] For a general trochoidal motion, the base circle and rolling circle have different radii.

[‡] The angular velocities are all measured relative to the fixed coordinates.

This can be interpreted as the locus generated by an N-bar linkage, with bar lengths $NR, \binom{N}{2}R^2, \ldots, R^N$—the first bar rotates with angular velocity 1 about the point 1, the second rotates with angular velocity 2 about the end point of the first bar, etc. Finally, the N-th bar rotates with angular velocity N about the end of the $(N-1)$-th bar, and its free end traces the trajectory (5.3). This is an example of a *higher trochoidal motion*, and the locus (5.3) is thus called a *higher trochoid*. Trochoidal motions, and the loci they generate, have been extensively studied by Wunderlich [31].

The ratios of (relatively prime) successive angular velocities, in the present case $1 : 2 : \cdots : N$, is called the *characteristic* of a trochoidal motion. Note also that the curve (5.3) can be generated by N different higher trochoidal motions. Different orderings of the N terms in (5.3) correspond to different physical N-bar linkages. We may regard the first $N - 1$ bars as defining a "moving system," in which the last bar rotates with uniform angular velocity. Clearly, the moving system is independent of the ordering of the initial $N - 1$ bars, but the final motion does depend on which of the N terms was chosen as the last. The N-fold generation of a higher trochoid by N distinct higher trochoidal motion is a generalization of the well-known double generation of a trochoid by the rolling motion of a circle on another circle.

If all entries of the characteristic are integers, the resulting higher trochoid is a rational curve—the algebraic order is, in general, twice the maximum absolute value in the characteristic. Hence, our curves are of order $2N$. From [31] we may also infer that these curves have N-fold points at the circular points at infinity, $(W, X, Y) = (0, 1, \pm i)$, as their only points at infinity.

In the theory of higher trochoids, the so-called *cycloidal trochoids* play a distinguished role. These curves can also be generated as the envelope of a line that executes a higher trochoidal motion. We mention just a few of their remarkable properties: their evolutes and all their offsets are also cycloidal trochoids, and their arc lengths admit closed-form expressions in terms of trigonometric functions. Since higher trochoids with only integer entries in the characteristic are rational, cycloidal trochoids with integer characteristics are examples of *rational curves with rational offsets* [28].

Cycloidal trochoids with $N = 2$ are called epicycloids and hypocycloids. In the case of the Minkowski square of a circle that passes through the origin (i.e., $R = 1$) we obtain the cardioid as a special instance of the epicycloid. It is not difficult to see that, when $R = 1$, the curve (5.3) is a cycloidal trochoid for any N. If $\mathbf{c}(\varphi) = r(\varphi)e^{i\varphi}$ is the polar form (with respect to the origin) of the circle $1 + e^{i\theta}$, we have $\theta = 2\varphi$, and the angle between the normal $\mathbf{n}(\varphi)$ to the circle and its position vector $\mathbf{c}(\varphi)$ is also φ (Figure 10). Upon forming the N-th power, $\mathbf{z}(\varphi) = \mathbf{c}^N(\varphi)$, the polar angle becomes $N\varphi$, and the normal at $\mathbf{z}(\varphi)$ is thus at angle $(N + 1)\varphi$ with the real axis (Figure 10). Hence, the tangent line at "time" φ can be parameterized by a real variable λ as
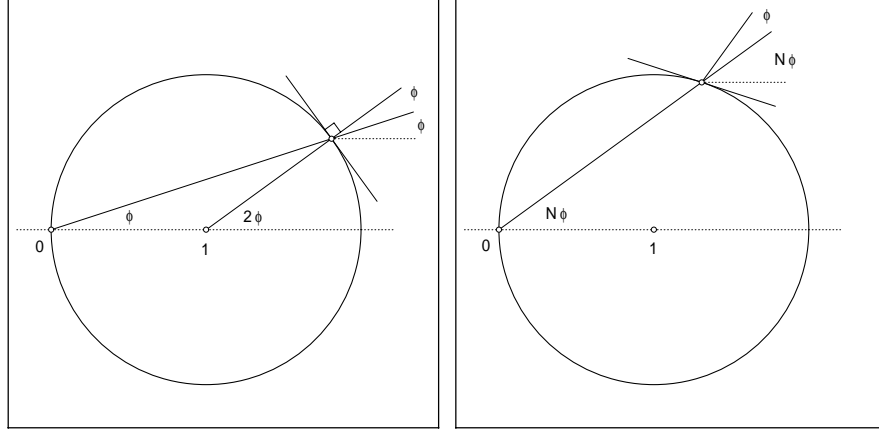
Figure 10. Left: polar form $\mathbf{c}(\varphi)$ of the circle $1 + e^{i\theta}$ with respect to the origin—the normal makes angle φ with the position vector. Right: the normal to the N-th power $\mathbf{c}^N(\varphi)$ of this circle makes angle $(N + 1)\varphi$ with the real axis.

$$\mathbf{z}(\lambda) = \sum_{k=0}^{N} \binom{N}{k} e^{i2k\varphi} + i\lambda\, e^{i(N+1)\varphi}. \tag{5.4}$$

This shows that the tangent is executing a trochoidal motion of $N + 1$ steps, with characteristic $2 : \cdots : 2N : N + 1$. However, choosing a suitable function

$$\lambda(\varphi) = a\sin m\varphi = a\,\frac{e^{im\varphi} - e^{-im\varphi}}{2i},$$

we can eliminate one of the first N terms in (5.4), and thus obtain a generation of $\mathbf{z}(\varphi)$ as the envelope of a line undergoing a trochoidal motion of N steps.

The description of N-th Minkowski powers of circular disks as sets bounded by higher trochoids offers an elegant counterpart to the characterization [9] of N-th Minkowski roots of circular disks as sets bounded by generalizations of the well-known *oval of Cassini* [19], [21]—see [9] for complete details.

6. Closure

An exact parameterization for the boundary of a general Minkowski product of N circular disks in the complex plane has been derived, that is sufficiently tractable to be of practical use in applications where *exact* operations (rather than containment results) on complex sets are required. Apart from rational arithmetic, evaluating this parameterization entails only the sine and cosine of a single angular variable and the extraction of N real square roots. Many basic set operations (point membership, union and intersection, etc.) become feasible by means of this representation. However, the detailed elaboration of such algorithms warrants a separate substantive study.

Since Cartesian ovals may be *defined* as the boundaries of the Minkowski product of two circles [12], the loci given by (4.2) are natural "higher-order" generalizations of Cartesian ovals. This perspective raises several interesting questions concerning the manner in which the subtle geometry of Cartesian ovals, summarized in Section 2, generalizes to the curves (4.2). For example: are the curves (4.2) also anallagmatic—and, if so, with respect to which circles of inversion? One might also expect[*] these curves to admit simple descriptions, analogous to (2.1)–(2.2), in terms of a system of *multipolar coordinates* [10] with respect to poles at $0, a_1, ..., a_N$. However, preliminary investigations reveal that such equations cannot be linear or quadratic.

Acknowledgement

References

1. Alefeld, G. and Herzberger, J.: *Introduction to Interval Computations*, Academic Press, New York, 1983.
2. Boltyanskii, V. G.: *Envelopes*, Macmillan, New York, 1964.
3. Brannan, D. A., Esplen, M. F., and Gray, J. J.: *Geometry*, Cambridge University Press, 1999.
4. Bruce, J. W. and Giblin, P. J.: *Curves and Singularities*, Cambridge University Press, 1984.
5. Chapellat, H., Bhattacharyya, S. P., and Dahleh, M.: Robust Stability of a Family of Disc Polynomials, *International Journal of Control* **51** (1990), pp. 1353–1362.
6. Coolidge, J. L.: *A Treatise on the Circle and the Sphere*, Clarendon Press, Oxford, 1916.
7. Farouki, R. T. and Chastang, J.–C. A.: Curves and Surfaces in Geometrical Optics, in: Lyche, T. and Schumaker, L. L. (eds), *Mathematical Methods in Computer Aided Geometric Design II*, Academic Press, 1992, pp. 239–260.
8. Farouki, R. T. and Chastang, J.–C. A.: Exact Equations of "Simple" Wavefronts, *Optik* **91** (1992), pp. 109–121.
9. Farouki, R. T., Gu, W., and Moon, H. P.: Minkowski Roots of Complex Sets, in: *Geometric Modeling and Processing 2000*, IEEE Computer Society Press, 2000, pp. 287–300.
10. Farouki, R. T. and Moon, H. P.: Bipolar and Multipolar Coordinates, in: Cippola, R. (ed.), *The Mathematics of Surfaces IX*, Springer, 2000, pp. 348–371.
11. Farouki, R. T., Moon, H. P., and Ravani, B.: Algorithms for Minkowski Products and Implicitly-Defined Complex Sets, *Advances in Computational Mathematics* **13** (2000), pp. 199–229.
12. Farouki, R. T., Moon, H. P., and Ravani, B.: Minkowski Geometric Algebra of Complex Sets, *Geometriae Dedicata* **85** (2001), pp. 283–315.
13. Gargantini, I. and Henrici, P.: Circular Arithmetic and the Determination of Polynomial Zeros, *Numerische Mathematik* **18** (1972), pp. 305–320.
14. Gomes Teixeira, F.: *Traité des Courbes Spéciales Remarquables Planes et Gauches*, Tome I, Chelsea (reprint), New York, 1971.
15. Hahn, L.–S.: *Complex Numbers and Geometry*, Mathematical Association of America, Washington, D.C., 1994.
16. Hauenschild, M.: Arithmetiken für komplexe Kreise, *Computing* **13** (1974), pp. 299–312.
17. Hauenschild, M.: Extended Circular Arithmetic, Problems and Results, in: Nickel, K. L. E. (ed.), *Interval Mathematics 1980*, Academic Press, New York, (1980), pp. 367–376.

---

[*] For example, the n-th Minkowski root of a complex disk is a multipolar generalization of the ovals of Cassini, the poles -1 and $+1$ being replaced by the n-th roots of unity [9].

18. Henrici, P.: *Applied and Computational Complex Analysis*, Vol. I, Wiley, New York, 1974.
19. Lawrence, J. D.: *A Catalog of Special Plane Curves*, Dover, New York, 1972.
20. Lin, Q. and Rokne, J. G.: Disk Bézier Curves, *Computer Aided Geometric Design* **15** (1998), pp. 721–737.
21. Lockwood, E. H.: *A Book of Curves*, Cambridge University Press, 1967.
22. Moore, R. E.: *Interval Analysis*, Prentice Hall, Englewood Cliffs, 1966.
23. Moore, R. E.: *Methods and Applications of Interval Analysis*, SIAM, Philadelphia, 1979.
24. Needham, T.: *Visual Complex Analysis*, Oxford University Press, 1997.
25. Pedoe, D.: *Geometry: A Comprehensive Course*, Dover, New York, 1970, reprint.
26. Petković, M. S. and Petković, L. D.: *Complex Interval Arithmetic and Its Applications*, Wiley-VCH, Berlin, 1998.
27. Polyak, B. T., Scherbakov, P. S., and Shmulyian, S. B.: Construction of Value Set for Robustness Analysis via Circular Arithmetic, *International Journal of Robust and Nonlinear Control* **4** (1994), pp. 371–385.
28. Pottmann, H.: Rational Curves and Surfaces with Rational Offsets, *Computer Aided Geometric Design* **12** (1995), pp. 175–192.
29. Ratschek, H. and Rokne, J.: *Computer Methods for the Range of Functions*, Ellis Horwood, Chichester, 1984.
30. Schwerdtfeger, H.: *Geometry of Complex Numbers*, Dover, New York, 1979.
31. Wunderlich, W.: Höhere Radlinien, *Österreichisches Ingenieur-Archiv* **1** (1947), pp. 277–296.
32. Zwikker, C.: *The Advanced Geometry of Plane Curves and Their Applications*, Dover, New York, 1963.